ELSEVIER

Contents lists available at ScienceDirect

Ecotoxicology and Environmental Safety

journal homepage: www.elsevier.com/locate/ecoenv





Evaluation, optimization study, and life cycle assessment of novel eco-friendly PVA-based nanocomposite hydrogel adsorbents for methylene blue and paracetamol removal

Noha A. Elessawy ^{a,*}, Abdulrahman G. Alhamzani ^b, Sondos A.J. Almahmoud ^b, Benjamin S. Hsiao ^c

- ^a Computer Based Engineering Applications Department, Informatics Research Institute IRI, Alexandria 21934, Egypt
- ^b Chemistry Department, College of Science, Imam Mohammad Ibn Saud Islamic University (IMSIU), Riyadh 11623, Saudi Arabia
- ^c Department of Chemistry, Stony Brook University, Stony Brook, New York, NY 11790, United States

ARTICLE INFO

Edited by Dr. G. Liu

Keywords: Hydrogel Poly (vinyl alcohol) Palm fronds Water purification Paracetamol removal Dye removal

ABSTRACT

In this study, an eco-friendly and novel hydrogel based on a crosslinked polyvinyl alcohol (PVA), iota carra $geen an \ (IC) \ and \ polyvinylpyrrolidone \ (PVP) \ scaffold, \ containing \ a \ large \ amount \ (10-50 \ wt\%) \ of \ nanoscale \ palm$ fronds (NPF) as additives, for water purification was demonstrated. A life cycle assessment (LCA) findings on NPF as biomass waste incorporated into PVA_PVP_IC polymer matrix was presented, and the results highlight the necessity of focused actions to reduce environmental impact and support the palm waste utilization in a sustainable manner. The multicomponent nanocomposite hydrogels were examined as adsorbents in a system work in batches for methylene blue (MB) and paracetamol (PCT) removal. The results show that, the presence of NPF, which dispersed in the hydrogel PVA_PVP_IC scaffolds containing both covalent and non-covalent cross-linking bonds, greatly enhanced the MB and PCT adsorption efficiency. A response surface methodology (RSM) model was used to find the best operating parameters of contaminant adsorption, including time, adsorbent dose, and starting concentration of pollutants. By using this statistical model, it was found that the optimal conditions for the adsorption reaction to achieve the complete removal of MB are 66.7 h adsorption time duration, 98.5 mg $\rm L^{-1}$ starting concentration, and an adsorbent dose of 5.9 mg, while for the complete removal of PCT, it is 57.6 h adsorption time duration, 80 mg L^{-1} starting concentration, and an adsorbent dose of 6 mg. The reusability of the nanocomposite hydrogels were tested for 5 cycles, all showed high adsorption capacity, indicating the potential for practical application of this nanocomposite hydrogel system. This study indicates that the prepared nanocomposite hydrogel raises the standard used for treatment of wastewater and also gives a solution to protect the environment and mitigate global warming.

1. Introduction

Due to the rapid industrialization, many natural water resources have been polluted with all kinds of contaminants including dyes, heavy metals, pharmaceutical chemicals, pesticides and fertilizers that cause serious health issues. One of the most industrial water pollution issues involving dyes such as methylene blue (MB), which has carcinogenic properties to humans (Peighambardoust et al., 2022; Toghan et al., 2023). Additionally, this dye poses a risk for aquatic life because it blocks sunlight's ability to penetrate in water that may impede photosynthesis and limit the growth of aquatic biota. Furthermore, this dye

can break down anaerobically with bacteria where the incomplete degradation can produce toxic amines (Weber and Wolfe, 1987). Meanwhile, the water pollution as a result of the existence of pharmaceutical residues at high concentrations is another water pollution issues. In this scenario, paracetamol (PCT) was chosen as a model medication contaminant used to treat fever and mild to moderate pain. PCT is extremely soluble in water (Romdhani et al., 2023). In the last three years from the beginning of Covid 19 pandemic, it was found that the concentration of PCT residue in sewer systems was increased because it could be excreted through the urine of humans under medical treatment. Additionally, it is occasionally unlawfully emitted by some

E-mail address: nony_essawy@yahoo.com (N.A. Elessawy).

^{*} Corresponding author.

industrial manufacturers when the drugs become expired or unneeded (Shaheen et al., 2022). Most of these organic pollutants may already be eliminated using various physical and chemical water treatment methods. These methods include of filtration, adsorption, photocatalysis, and advanced oxidation processes (AOPs) (Elessawy et al., 2020; Pooladi et al., 2021; Rashid et al., 2021; Toghan et al., 2023; Xu et al., 2018). The adsorption approach is more cost-effective among these techniques because of its simplicity of usage in a large-scale setup, and relatively low cost (Rashid et al., 2021).

Recently, researchers are paying close attention to the utilization of natural lignocellulosic biowastes and agricultural wastes as adsorbents in wastewater treatment (Alizadeh et al., 2022; Foroutan et al., 2017). However, date palm is the Middle East's most widely widespread palm (Faiad et al., 2022). A little portion of this waste may be used as animal feed, while most of this waste is left to decompose naturally and used as fertilizer. Regrettably, the majority of the date palm waste is burned on fields or dumped in landfills, which seriously pollutes the environment in nations that produce dates. Due to the low moisture level and the significant amount of volatile solid of date palm waste, a variety of physiochemical and biochemical processes are available for its sustainable usage (Saud et al., 2023). In specific, date palm waste can be used as an economically viable raw material for developing new adsorbent materials for pollution remediation (Salem et al., 2021; Saud et al., 2023; Sizirici et al., 2021; Tahir et al., 2020).

On the other hand, it has been shown that a number of environmentally acceptable polymers with synthetic and natural sources may be used to purify water. For instance, iota carrageenan (IC), which is derived from red seaweed, each disaccharide unit contains two sulfated groups. Owing to its natural abundance and chemical utility, it is used widely to remove organic contaminants, including pharmaceutical pollutants (Gouda et al., 2021a). Other examples involve the use of polyvinyl alcohol (PVA) and polyvinylpyrrolidone (PVP) synthetic polymeric materials. They have been considered as biodegradable, water soluble and non-toxic polymers (Ghosh et al., 2022; Wu et al., 2023). Since of its OH functional groups, PVA is commonly used to remove different water pollutants since they have the potential to chemically crosslink and provide extremely hydrophilic and water stability qualities. In this study, we consider the combination of PVA with IC and PVP and create a porous and interpenetrated network that is rich in sulfate and hydroxyl groups, which might be useful for enhancing the capacity of adsorption (Elessawy et al., 2022; Gouda et al., 2019; Ye et al., 2012) as well as for hosting other nanoscale adsorbents.

The three-component network scaffold (PVA_PVP_IC) can be used to create hydrogels with excellent responsiveness, softness, anti-fouling,

and biocompatibility (Ahmed, 2015; Correa et al., 2021; Liu et al., 2020). These properties of the hydrogel, in combination with abundant functional groups, can enable the prepared scaffold to be used as an adsorbent hydrogel in wastewater purification (Bashir et al., 2020; Tran et al., 2018). We extensively use PVA, a hydrophilic polymer, to prepare hydrogels due to its strength, pH stability, and processibility. As it is highly soluble in water, it is often chemically crosslinked to become a water-resistant network structure. The second component of PVP is the most popular pH-responsive polymer, which can offer the hydrogel stimuli-responsive properties (Chang et al., 2023). The third component of IC is a natural polysaccharide, which can also be used as a scaffolding material to create hydrogel. However, to increase the adsorption capability, we further investigate the use of the PVA PVP IC scaffold to host nanoscale bio-adsorbent particles derived from the waste of date palm. Adsorbents derived from different parts of palm trees for water treatment and their performance comparisons with nanocellulose are illustrated in Table 1.

In this study, nanoscale date palm frond (NPF) waste was chosen as the bio-adsorbent additive, which was added to the PVA, IC, and PVP green ternary scaffold at different loading contents to obtain a novel ecohydrogel adsorbent composite that can be used in wastewater treatment depending on the concept of "waste treat waste" which combines water treatment with solid waste management in order to improve the development of bilateral policies in the area of sustainability and allow treated waters to be used for various purposes. To test the removal efficiency of PVA_PVP_IC_NPF composite hydrogel, two organic compounds, such as MB and PCT were chosen as model contaminants for the batch adsorption studies. Furthermore, a possible mechanism for the PVA PVP_IC_NPF composite hydrogel's adsorption of PCT and MB dye was suggested. In addition, the response surface methodology (RSM) model was applied to determine the ideal values of the most important factors in the adsorption process, and reusability in adsorption was evaluated.

2. Materials and methods

2.1. Preparation of PVA PVP IC NPF nanocomposite hydrogels

2.1.1. Materials

PVA (Sigma-Aldrich, medium MW, 99 % hydrolysis), IC (Sigma-Aldrich, USA), PVP (Acros Organics, USA), Ethanol 100 % (Sigma-Aldrich, USA), Glutaraldehyde (GA) (25 wt% in $\rm H_2O$, Sigma-Aldrich, USA)

Table 1Adsorbents derived from different palm tree waste and their removal efficiency against varying contaminants.

Adsorbent	Adsorbate	Efficiency (%)	Adsorption capacity (mg/g)	Ref.
Carbon nano-crystal/ polyamide thin-film composite	oil spill	97.45	-	(Saud et al., 2023)
Biochar produced from date seed biomass	Pb^{2+}	55	-	(Mahdi et al., 2018)
Date palm trunk fibers	Cd^{2+}	-	54.57	(Al-Ghamdi et al., 2013)
Date palm fibers	Cu ²⁺	~ 88	-	(Amin et al., 2016)
	As^{5+}	~ 70	-	
	Pb^{2+}	~ 81	-	
Date seed ash	B^{3+}	47	-	(Al Haddabi et al., 2016)
Activated date pits	MB	-	220	(Ashour, 2010)
•	Remazol dyes	-	164	
NaOH chemically modified date palm fiber	phenol	86	-	(Siva Kumar et al., 2023)
(DPF600)	phenol	64	15.93	(Fseha et al., 2023)
Modified date palm leaf (DPL) waste	2,4-Dichlorophenoxyacetic acid (2,4-DPA) herbicide	72.6	-	(Rambabu et al., 2023)
Nano-activated date pits	organophosphate pesticide (profenofos)	100	-	(Hassan et al., 2020)

2.1.2. Method

The following procedures were used to prepare the hydrogel nano-composite (Fig. 1); to make a clear solution, PVA was dissolved at 90 $^{\circ}$ C in DW for two hours while being vigorously stirred. This yielded a 10 wt percent PVA solution. By stirring 2 wt percent IC in 50 mL DW acidified with 1 mL of acetic acid, IC clear solution was produced. By dissolving 2 wt percent of PVP in fifty milliliters of a 50:50 vol% water: ethanol combination at room temperature. Then mixing PVA, IC, and PVP solutions and stirred for 2 h to produce PVA, IC, and PVP solution. The PVA:IC:PVP blend's weight percentage was around 70:15:15.

The preparation of NPF was as follows. The palm frond samples were first collected, washed, and then dried for 24 h at 60 °C. The dried palm frond samples were subsequently shredded to fine powder then grinded into nanoscale particles (particle size was about 600 μm) using ball milling at 500 rpm for 15 min. For composite hydrogel preparation, different concentrations of NPF (10–50 wt%) were added as a suspension in acetone to the PVA_PVP_IC solution, and the stirring was done to the mixture for 2 h. The composite mixture was subsequently cross-linked by adding 3 mL of GA, where the mixture was thorough stirring for 10 min at 40 °C to form the nanocomposite hydrogel. The formed hydrogel with different NPF concentrations were named PVA_PV-P_IC_10NPF, PVA_PVP_IC_20NPF, PVA_PVP_IC_30NPF, PVA_PVP-P_IC_40NPF, and PVA_PVP_IC_50NPF, respectively.

2.2. Characterization of NPF and nanocomposite hydrogels

The produced NPF powder and the PVA_PVP_IC_NPF hydrogels underwent some basic characterization, including Fourier Transform Infrared (FTIR, Shimadzu FTIR-8400 S- Japan). Using scanning electron microscopy (SEM) Model: JEOL 6360LA), the morphologies of the palm frond nanoparticles and nanocomposite hydrogels were examined. Bettersize Instruments Ltd was used to measure the size distribution of the NPF. A Malvern Nanosizer zeta potential was used to measure the zeta potential for hydrogel samples.

2.3. Swelling capacity

In this experiment, a beaker containing a known volume of dried nanocomposite hydrogel was filled with various volumes of DI water at room temperature. The weight of the swelled hydrogel was determined for the swelling test at various intervals (the test was ended when the sample weight reached a consistent value). After the enlarged hydrogel was taken out, a paper towel was used to remove any remaining water from the hydrogel's surface. After that, a digital balance was used to weigh the hydrogel (W), and the equilibrium swelling ratio (Se) was computed using the subsequent relation:

$$Se(\%) = [(W_d - W_s)/W_d] \times 100$$
 (1)

2.4. Evaluation of the adsorption efficiency

A batch equilibration method was utilized to conduct the adsorption results. A range of MB and PCT concentrations (50–150 mg $\rm L^{-1})$ were used. The main characteristics of the MB and PCT molecules are shown in Table S1 (Supplementary Data). The pH values of the solutions were changed using 0.1 M NaOH and 0.1 M HCl. Using the UV–visible spectroscopy, the concentrations of MB and PCT in the solution were measured at wavelengths of 650 nm and 245 nm, respectively. The following formulas were used to determine the adsorbed quantities

$$q_t = \frac{C_0 - C_t}{m} V \tag{2}$$

$$q_e = \frac{C_0 - C_e}{m} V \tag{3}$$

where q_t and q_e (mg g $^{-1}$) are the amounts of the MB or PCT molecules adsorbed per unit weight of the nanocomposite hydrogel at time t and equilibrium, respectively; The MB or PCT concentrations at the start time, time t, and equilibrium time are represented by the values C_0 , C_t , and C_e (mg L $^{-1}$)., respectively. V (L) is the volume of MB or PCT solution; m (g) is the mass of nanocomposite hydrogel. Removal efficiency (R%) was calculated according to the following equation:

$$R\% = \frac{C_0 - C_t}{C_0} \times 100$$
 (4)

The pH value was set at 7 and the adsorption period was varied within a range of 2 h to 48 h and temperatures 25–45 $^{\circ}$ C for kinetics, isotherm and thermodynamics studies.

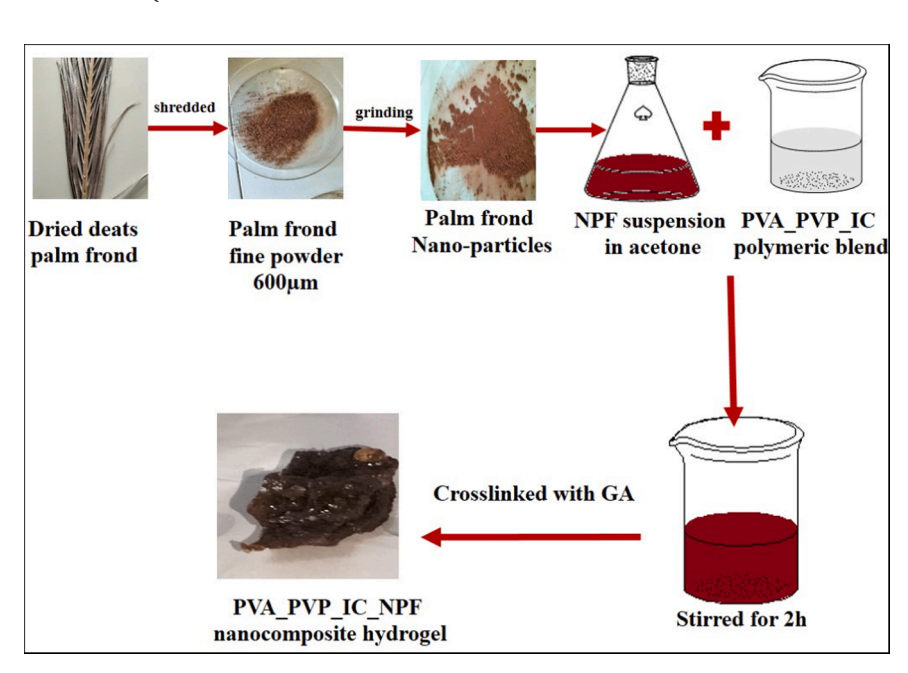


Fig. 1. Fabrication procedures to prepare PVA_PVP_IC_NPF nanocomposite hydrogel.

2.5. Adsorption process optimization

We aimed to use a response surface methodology model (RSM) to create a link between the components and the related attributes in order to improve the adsorption process. The response surface approach's selected matrix, after 17 trials, complied with the Box–Behnken design (Box and Behnken, 1960; Marton et al., 2022). As shown in Table S2 for MB and PCT pollutants, three variables were employed to assess the adsorption performance: A (time, min.), B (starting concentration, mg $\rm L^{-1}$), and C (adsorbent dosage, mg), at three levels of -1, 0, and 1. Design-Expert, 13.0.9.0 software from STAT-EASE, INC were used.

2.6. Regeneration and recycling

To examine the ability of the nanocomposite hydrogel to regenerate, 1 g of PVA_PVP_IC_NPF nanocomposite hydrogel was added to a conical

flask containing 25 mL of 50 mg $\rm L^{-1}$ MB solution and another one containing 25 mL of 50 mg $\rm L^{-1}$ PCT solution. The mixture was shaken at 150 rpm for 48 h. After the adsorption process, the nanocomposite hydrogel was separated by filtration, then the mixture of hydrogel with 100 mL of ethanol and 10 mL of 0.1 M NaOH solution was sonicated for 12 h. Subsequently, the regenerated hydrogel was filtered, washed and then dried at 40°C for 4 h for the reuse study. The concentration of the filtered fluid was also measured. For typical regeneration process, the above procedures were repeated five times to treat the spent hydrogel.

2.7. Life cycle assessment

The current study's Life Cycle Assessment (LCA) was carried out within the framework of the ISO 14040 standard. OpenLCA 1.9, an open-source program, was used to perform the LCA. The databases Ecoinvent 3.4 and Agribalyse 3.0 were utilized, and the data was

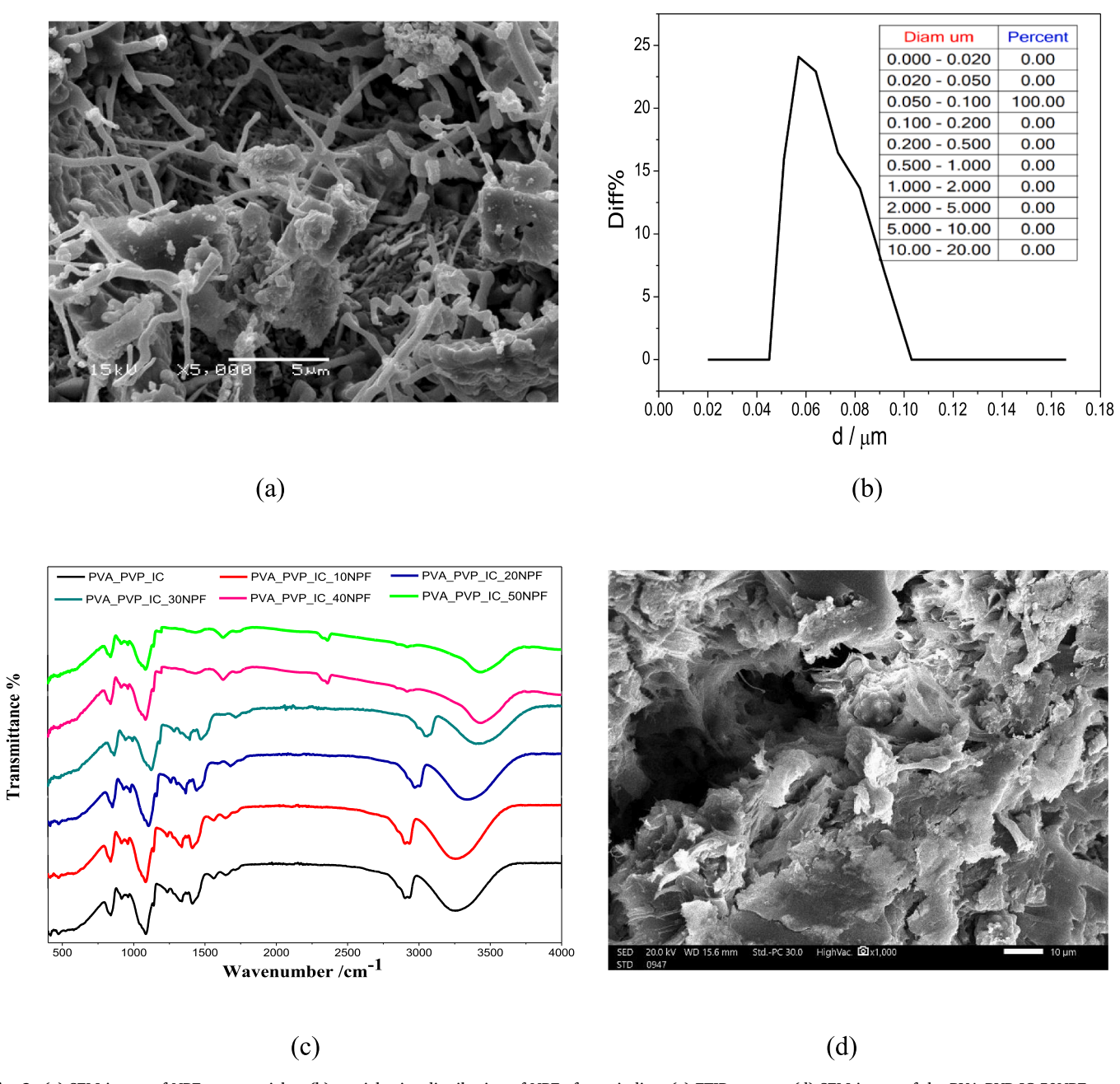


Fig. 2. (a) SEM image of NPF nanoparticles, (b) particle size distribution of NPF after grinding. (c) FTIR spectra, (d) SEM image of the PVA_PVP_IC_50NPF nanocomposite hydrogel.

interpreted using the ReCiPe 2016 (Marton et al., 2022) Midpoint (H) approach. Both the external data and the energy consumption came straight from the development that was done. It was taken into consideration to incorporate the impact of palm debris, which were burned when they weren't mixed into hydrogel. For the purposes of this LCA analysis, the processing of one kilogram of waste biomass from palm fronds was chosen as the functional unit. The system boundary did not include the transportation of palm waste; instead, it included the amount of energy and water needed to produce the NPF in a lab setting. As a result, the examination of the raw palm waste's reception through the grinding process' completion is included in the LCA scope. The primary LCA study outlined the grinding of raw palm waste as one of the primary unit processes. Producing NPF from raw date palm waste is depicted in Fig. S1 (supplementary information) in with the associated input and output components.

3. Results and discussion

3.1. Characterization of NPF and nanocomposite hydrogel

Samples of palm fronds were collected from a nearby date palm plantation and the compositions of a typical dried date palm frond are cellulose (27.3 %), hemicellulose (0.7 %), while lignin (8.4 %). Most of the oxygen functional groups are found in the components of hemicellulose and cellulose (Ahmad et al., 2012) which have a favorable impact on the cation adsorption process. However, the SEM image of NPF in Fig. 2a shows that, the palm frond samples after grinding are nanoscale particles, with a particle size distribution (determined by the Bettersize Instruments Ltd) illustrated in Fig. 2b.

The properties of PVA_PVP_IC nanocomposite hydrogel containing different weight ratios of NFP were first investigated using FTIR to investigate the material's functional groups, where the results are shown in Fig. 2c. The PVA_PVP_IC and PVA_PVP_IC_NPF hydrogels' FTIR spectra display a board band in the range of 3078–3470 cm⁻¹, which is indicative of the PVA's stretching -OH groups (Gouda et al., 2022). With the increase of the NPF content, this band was shifted to a higher wavenumber, suggesting that NPF had completely dispersed into the polymeric scaffold. In addition, the intensity of the peak decreased with increasing the NPF content from 10 % to 50 %. It can be explained as the hydrogel with more OH functional groups can easily absorb the water molecule onto its surface (Khiewsawai et al., 2023). Furthermore, two bands overlap at around 2900 cm⁻¹ became apparent, which can be explained as the result of the C-H stretching from the polymer scaffold and the oxygen functional groups of PVA, IC, and PVP (Gouda et al., 2020a). The IC component exhibited distinctive bands at 845, 805, and 930 cm⁻¹, while the bands between 900 and 1200 cm⁻¹ could be attributed to IC's sulfonic groups (Gouda et al., 2020b).

The SEM morphology, as illustrated in Fig. S2, demonstrated that the composite hydrogels for all samples had an open-framework structure that is microporous, facilitating the easy absorption of PCT and MB molecules on the hydrogel's internal active sites. Additionally, it was observed that the hydrogel's structure became more compact as the NPF content increased. Meanwhile, as seen by the SEM image displayed in Fig. 2d for the PVA_PVP_IC_50NPF sample, the structure resembles slender threads connecting one another throughout the entire network.

From the previous it was concluded that the cross-linking process for making a relatively homogeneous nanocomposite network, which involves both chemical and physical interactions between NPF and the PVA_PVP_IC polymeric matrix, has successfully taken place, as evidenced by the FTIR analysis and by the observation of morphology. The resulting nanocomposite hydrogel provides both adsorbent characteristics as well as good mechanical stability and strength. Similar systems with good absorption properties and resilience to deterioration and durability have been demonstrated before (Gouda et al., 2021b; Gupta et al., 2024).

3.2. Swelling capacity

One key element influencing the effectiveness of adsorption is the hydrogel adsorbent's swelling capacity. The significant swelling capacity can improve the removal effectiveness by expanding the surface area that is available for adsorption (Khiewsawai et al., 2023). The results are shown in Fig. 3a. In PVA_PVP_IC_10NPF, its swelling ratio is significantly higher than that of PVA_PVP_IC (without NPF). This is because the presence of NPF enhance the hydrophilicity of the system due to the increase of the hydroxyl groups of cellobiose units in NPF (Salunkhe and Schuman, 2021).

Interestingly, the swelling ratio of PVA_PVP_IC_NPF hydrogels decreases with increase of the NPF amount (above 10 wt%) due to the increasing degree of crosslinking in hydrogel (Olad et al., 2020). This support the interactions (both physical and chemical) between NPF and polymer scaffold. At 40 wt% of NPF, the system shows a low swelling ratio, indicating that the NPF particles probably fill the hydrogel pores and create a compact and condensed structure, which was evident from TEM images (Fig. S2), and that reduces the swelling capacity significantly (Spagnol et al., 2012). It is also interesting to see that after immersing all hydrogels in distilled water, their swelling ratios increase significantly at first. After a rapid increase, the swelling ratio diminishes and only exhibits a gradual increase for each sample until a value of equilibrium has been achieved. It is found that the PVA_PVP_IC sample reaches the equilibrium after 10 h approximately, whereas it takes about 15 h for all nanocomposite hydrogels to reach their equilibrium values.

The effect of temperature (25–45 °C) on the swelling ratio of PVA_PVP_IC and PVA_PVP_IC_NPF hydrogels have also been investigated. The results are shown in Fig. 3b, where the swelling ratio of the hydrogel increases slightly as temperature rises. The explanation behind this phenomena is the low segmental mobility of the hydrogel chains at low temperatures, resulting in low swelling ratios. As the temperature rises, the hydrogel's swelling ratio rises due to the enhanced mobility of the polymer chains and the water molecules' rapid diffusion into the hydrogel scaffold (Mahdavinia et al., 2016).

3.3. Evaluation of the adsorption efficiency

At solution pH equal to 7 and adsorption time duration equal to 48 h with a pollutants initial concentration of 100 mg $\rm L^{-1}$, a batch adsorption process was conducted to investigate the effect of NPF at different concentrations in the PVA_PVP_IC hydrogel on the adsorption efficiency against MB and PCT. The results are shown in Fig. 4a & b, where the hydrogels' adsorption capacity is seen to increase with the NPF content up to 30 wt% and then decrease with higher NPF contents (i.e., 40 wt% and 50 wt%). The improved generation of hydrogen bonding and electrostatic attraction forces between the oxygenated groups in the PVA,IC, PVA NPF composite system and the functional groups in MB and PCT may be responsible for the increase in adsorption capacity with NPF concentration (< 30 wt%). The decrease in the adsorption capacity with NPF content (>30 wt%) can be explained by the decrease in swelling ratio of the system and thus the reduction of active surface area for adsorption (Olad et al., 2020; Spagnol et al., 2012). Therefore, the PVA_PVP_IC_30NPF hydrogel nanocomposite was selected as the best sample for examining the optimum condition for adsorption, kinetics, isotherm and thermodynamics studies. In all samples, the removal efficiency is found to increase dramatically at first, and then increase gradually to reach an equilibrium value (after 24 h for PCT and 36 h for MB). At the equilibrium state, a balance between desorption and adsorption of PCT or MB cations is taking place.

The solution' pH value also can play a significant role affecting the interaction between the adsorbent and adsorbate. This is because the pH value can influence the surface charge of both scaffolding material and contaminants in solution (the species can be protonated and deprotonated with pH changes). The effect of solution pH on the surface chemistry of the prepared nanocomposite hydrogel was thus

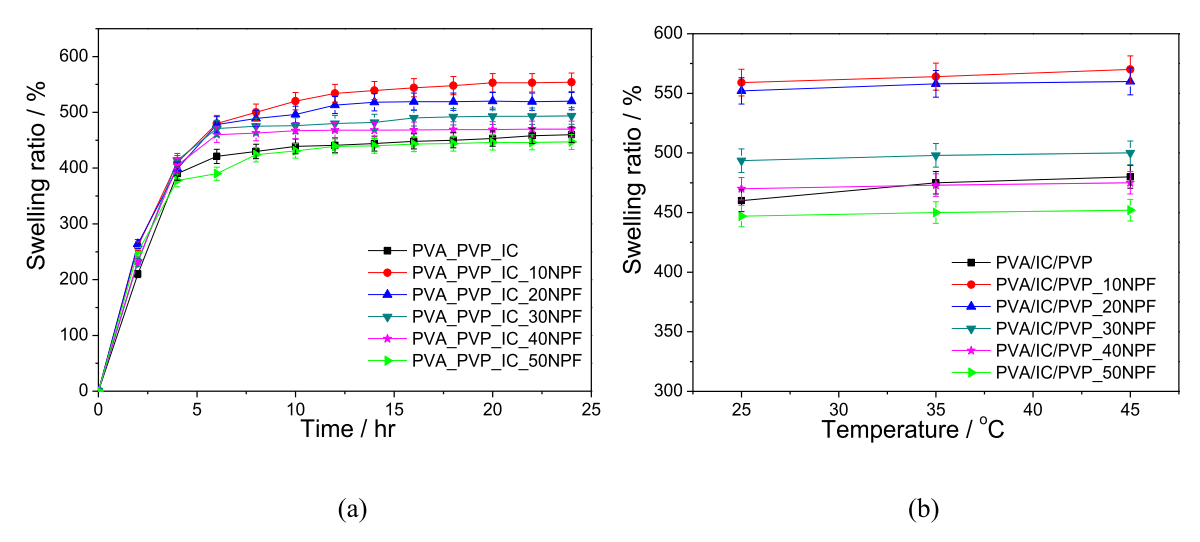


Fig. 3. (a) Swelling ratio % and, (b) effect of temperature on PVA_PVP_IC_NPF nanocomposite crosslinked hydrogels containing different concentrations of NPF at 10, 20, 30, 40, and 50 wt%.

investigated in the pH range from 2 to 12, where the zeta potential results are shown in Fig. 4c. It seen the nanocomposite hydrogels contain many negatively charged groups, and the zeta potential value becomes more negative with higher NPF content at higher pH value. In this case, the removal efficiency of organic cations is expected to increase when the pH increases. That was confirmed experimentally using the PVA_PVP_IC_30NPF nanocomposite hydrogel. The results are shown in Fig. 4d. It is seen that by increasing the solution pH from 2 to 12, the removal efficiency of MB by the PVA_PVP_IC_30NPF nanocomposite hydrogel increases. The explanation for this phenomenon might be that many hydronium ions surround the hydrogel surface at low pH values, and these ions can compete with MB cations. On the other hand, by increasing the pH, the carboxylic, sulfate and hydroxyl groups in the hydrogel of the nanocomposite can be ionized, which enhances the electrostatic contact between the MB cations and the hydrogel surface. However, for PCT, the adsorption process is found to decrease once pH increases above 7. This may be because the pKa value for PCT is 9.38. Thus, the OH groups can react with hydrogen ions that have been produced from PCT molecules at high solution pH levels, decreasing the surface's positive charge (Jozaghkar et al., 2022). In other words, at basic solution pH, dissociation of PCT molecules can occur (Fig. S3b in supplementary information), resulting in a rise in anionic species that push away the hydrogel nanocomposite's negative charge, reducing adsorption. This is seen in Fig. 4d, where the PCT uptake decreases at higher pH values. For the PVA PVP IC 30NPF nanocomposite hydrogel, the pH value of 7 appears to be the optimum condition for removing PCT, while the pH value of 12 seems to be the most effective condition for removing MB.

In order to determine the adsorption mechanism (chemisorption or physisorption), the PVA_PVP_IC_30NPF scaffold was investigated before and after MB and PCT adsorption by using FTIR analysis. By comparing the three spectra before and after adsorption, as shown in Fig. S4, it was noticed that there was a little change in the peaks. This means that chemical bonds were formed within the adsorption process. The change in the peak intensity can be attributed to the electrostatic interaction between the pollutants cationic molecules and OH ions that accumulated on the hydrogel surface. Consequently the adsorption of MB and PCT molecules on the PVA_PVP_IC_30NPF scaffold surface can result from a number of intermolecular interactions, whereas the electrostatic interaction and the Van der Waals force was likely to occur thus causing the adsorption on hydrogels to become physical adsorption. Furthermore, it is possible that the MB and PCT molecules will combine with the hydrogel's functional groups through hydrogen bond, and $\pi - \pi$ stacking between benzene rings, resulting to chemisorption. The likely

interactions are shown in Fig. 4e.

3.4. Optimization

The adsorption processes of the PVA_PVP_IC_30NPF nanocomposite hydrogel were optimized utilizing Box–Behnken design analysis. Three factors were chosen: the amount of adsorbent, the duration of the process, and the starting concentration of the pollutant (the process temperature was fixed at 25 $^{\circ}$ C). Quadratic dependency was assumed to represent the statistical link between the variables and the responses, namely removal % (Y), using the following equations:

$$Y_{MB} = 94+12.33A-9.5B+12.08 C+8.5AB-4.85AC+3.00BC-4.43A^2-1.58B^2-10.92C^2$$
 (5)

$$Y_{PCT} = 89+19.36A-6.62B+12.99 C+5.5AB+7.23AC-1.75BC-15.51A^2+1.51B^2-12.76C^2$$
 (6)

where A, B, and C are the experimental variables of the contact duration, starting MB or PCT concentration, and adsorbent dosage respectively (Table S3 and Table S5).

The findings of the Box-Behnken design analysis are presented in Fig. 5, which show a type of interaction that exists between the response (removal percentage) and the tested variables presented in 3D plots. For MB and PCT, it seems that removal effectiveness increases with increasing contact duration and adsorbent dosage, but falls with rising starting concentrations from 100 to 150 mg $\rm L^{-1}$. The findings show that the MB or PCT cations were adsorbed externally during the first stage of adsorption, when the rate of adsorption rose quickly.

For assessing the statistical significance of the quadratic response surface model, the common ANOVA approach was adopted. The high coefficient of determination R2 (0.9862) for MB and (0.9994) for PCT (Tables S4 and Table S6) of the quadratic model suggests that it fits the experimental data well (Foroutan et al., 2023a). According to the results, it was also found that the chosen quadratic model is significant because the obtained p values for MB and PCT are all less than 0.0001 (Foroutan et al., 2021) in addition the lower P-value indicated that, the adsorption duration time, the starting concentration of the pollutant and the amount of adsorbent had a significant effect on the removal %. Following this study, the ideal circumstances seemed to be as follows; 66.7 h adsorption time duration, 98.5 mg L⁻¹ starting concentration, and adsorbent dose of 5.9 mg to achieve the complete removal of MB (Fig. S5a); and 57.6 h adsorption time duration, 80 mg L^{-1} starting concentration and adsorbent dose of 6 mg for the complete removal PCT.

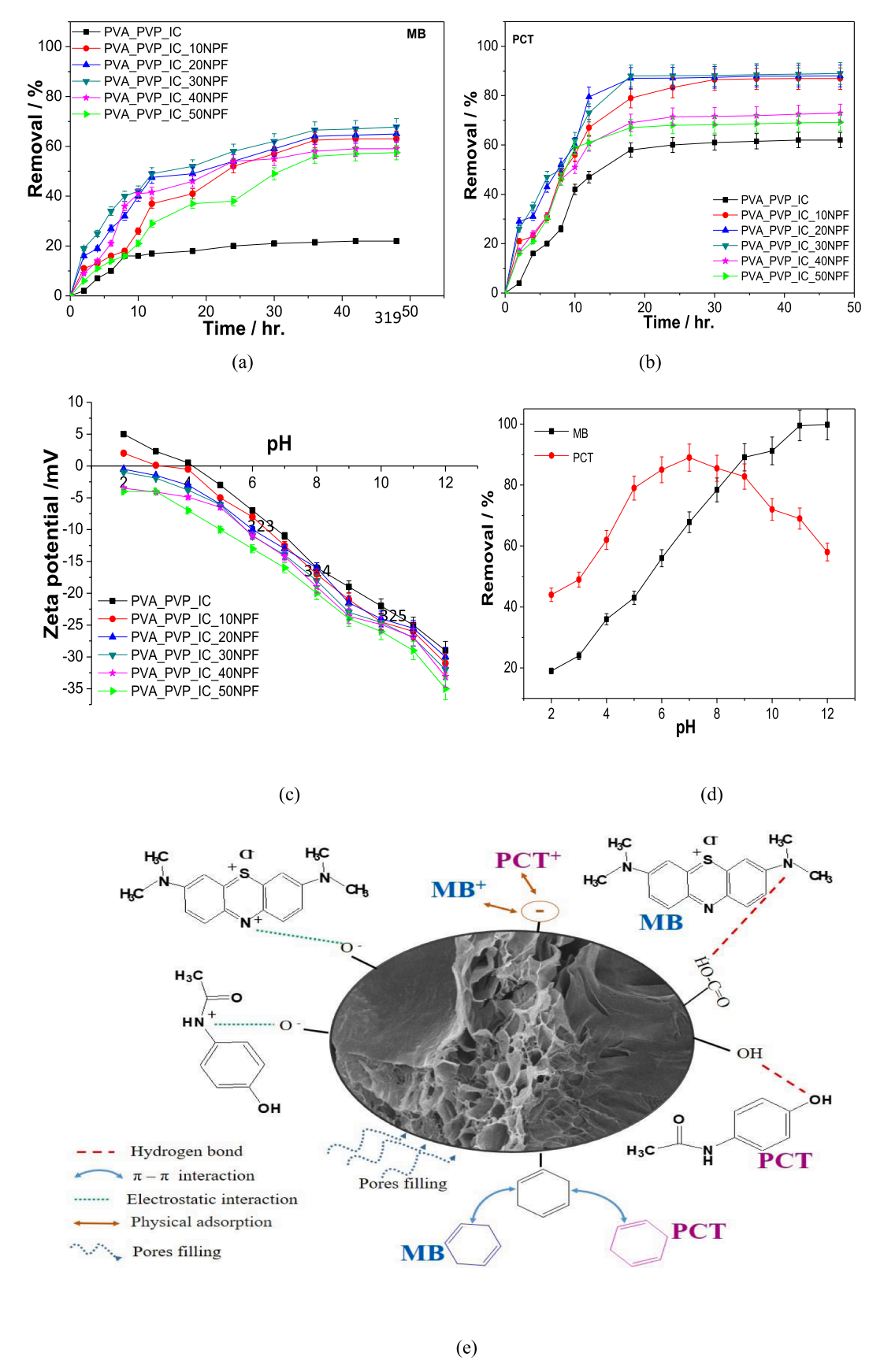


Fig. 4. The impact of contact duration and NPF concentration on (a) MB and (b) PCT adsorption process, (c) zeta potential, (d) effect of solution pH, and (e) possible intermolecular interactions for MB and PCT molecules for adsorption by the PVA_PVP_IC_30NPF hydrogel.

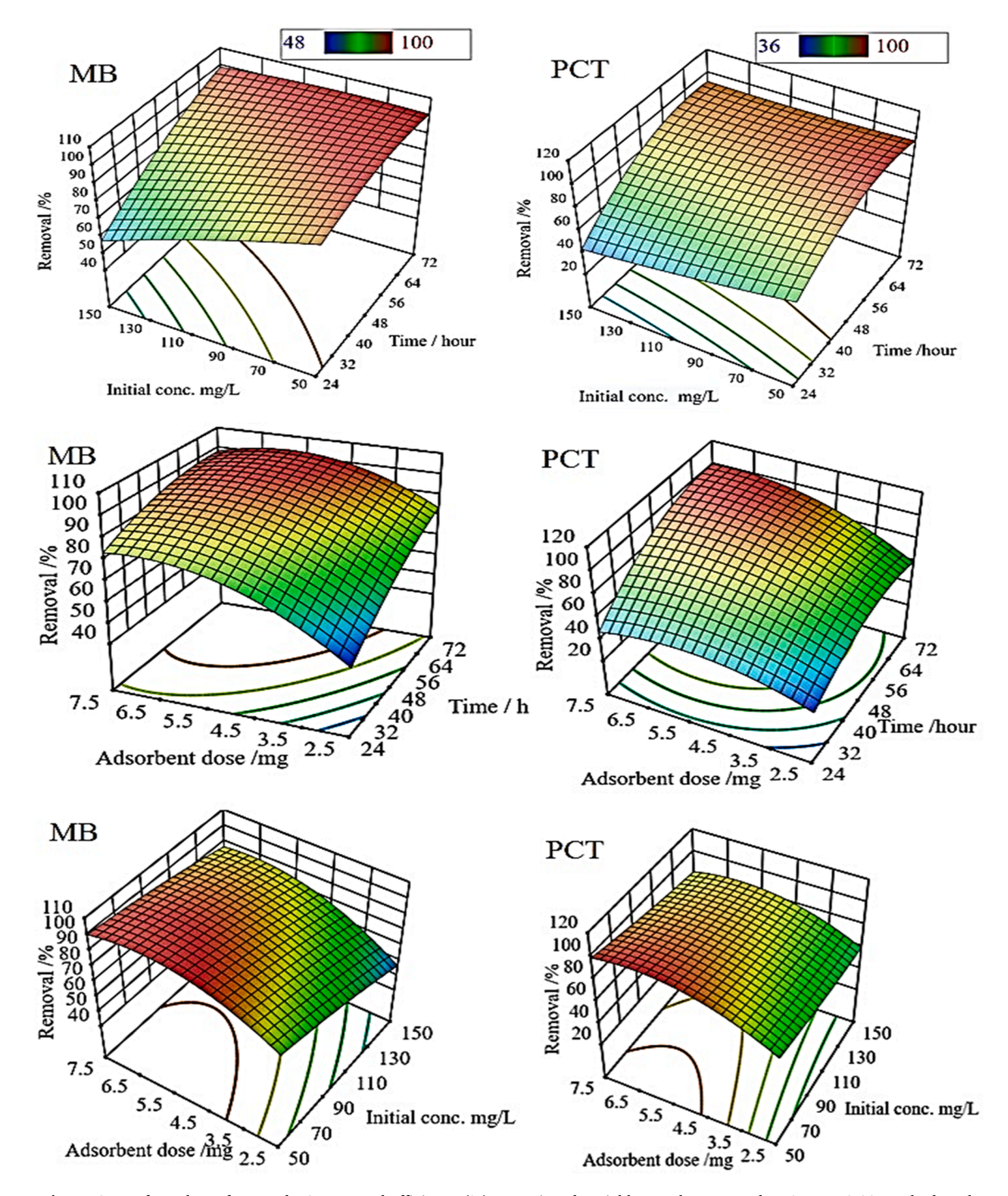


Fig. 5. 3D surface plots of MB and PCT removal efficiency (%) vs. assigned variables on the prepared PVA_PVP_IC_30NPF hydrogel.

Additionally, based on the perturbation plot, which facilitates comparing the impacts of every element at a specific location in the design space. Plotting the elimination percentage involves varying one element over its range while maintaining constant values for all other parameters. As seen in Figs. S5b & c, the reference point was placed at the midpoint (coded 0) of each component. However, the factor's high slope or curvature indicates that the reaction is sensitive to it. The insensitivity to changes in that specific element is indicated by a comparatively flat line. While the factors of adsorption time duration and adsorbent dose have a high effect on the removal efficiency (when they increase, the removal efficiency increases). It was also observed that the removal efficiency increases with increasing MB or PCT starting concentration before falling at high concentrations.

3.5. Adsorption kinetics, isotherm and thermodynamics

Using kinetic models (as illustrated in Table S7 in supplementary information file), we attempted to obtain a better comprehension of the adsorption process against MB and PCT using different starting concentrations of 50, 100, and 150 mg $\rm L^{-1}$, and at pH of 12 for MB and pH of 7 for PCT and temperature 25 °C, with 6 mg of PVA_PVP_IC_30NPF scaffold and solution volume of 50 mL. It was found that the MB adsorption reached equilibrium at 36 hr., and for PCT was 24 hr. The pseudo-first-order and pseudo-second-order models were used to fit this kinetic data; the corresponding plots and related parameters are shown in Table 2, Fig. S6 and Fig. S7. The findings show that the pseudo-second-order kinetic model well describes the adsorption process,

ΔS (J/mol.K)

Table 2
The kinetic and isothermal models parameters for MB and PCT adsorption onto PVA_PVP_IC_30NPF nanocomposite hydrogel at pH of 12 for MB and pH of 7 for PCT and temperature 25 °C; with 6 mg of the hydrogel and solution volume of 50 mL.

Starting concentrations (n	ng/L)						
	50		100			150	
	MB	PCT	MB		PCT	MB	PCT
q _{e,exp} (mg/g)	410	402	561		742	783	951
Pseudo-1st order							
q _{e'cal} (mg/g)	586	768	1824		788	761	1497
$k_1 (min^{-1})$	0.146	0.18	0.151		0.083	0.138	0.08
R ²	0.95	0.86	0.77		0.89	0.97	0.65
Pseudo–2 nd order							
q _{e,cal} (mg/g)	430	405	558		740	782	958
k ₂ (min ⁻¹)	0.002	0.002	0.0014		0.0011	0.0012	0.00
R^2	0.95	0.98	0.91		0.91	0.99	0.96
Intraparticle diffusion							
k _{i,1}	18.19	8.12	18.2		18.4	25.42	23.7
k _{i,2}	18.19	7.4	13.06		10.8	8.4	12.2
11,2	_	7.1	10.00		1010	0.1	12.2
k _{i,3}	3.23	6.7	7.77		8.1	7.4	4.39
Temperature °C							
remperature o		25 °C		35 °C		45 °C	
		MB	PCT	MB	PCT	MB	PCT
Langmuir isotherm							
q _m (mg/g)		724.6	1063	892	1121	1000	1198
k _L (L/mg)		0.73	0.26	1	0.34	1.24	0.42
		0.014	0.037	0.01	0.028	0.008	0.023
R_L R^2		0.995	0.997	0.998	0.999	0.995	1
Freundlich isotherm		*****	*****	*****	*****	*****	_
K _F (mg/g)		382.76	326.9	455.02	381.9	514.04	412.9
n		7.74	3.35	7.37	3.16	7.52	2.9
R^2		0.994	1	1	0.998	1	0.996
N Dubinin-Redushkovic isothe	rm isotherm isotherm	0.554	1	1	0.550	1	0.550
E (kJ/mol)	isotherm isotherm	15,500	12,900	14,900	12,913	13,800	12,451
B (mol ² /J ²)		2.07E-9	2.9E-9	2.25E-9	3E-9	2.63E-9	3.2E-
R ²		0.995	0.999	0.999	0.999	0.988	0.997
Temkin isotherm		0.555	0.555	0.555	0.555	0.500	0.557
b _T (kj/mol)		39.76	13.02	30.86	11.77	33.41	12.44
		693.96	4.24	242.47	4.42	965.2	7.82
A _T (L/g) R ²							
		0.995	0.998	0.997	0.989	0.996	0.995
ΔG (kJ/mol)		-6951.88	-10,433	-8311.38	$-12,\!430$	-9613.37	13,447
ΔH (kJ/mol)		32,713	34,631				

according to the surface kinetic model's determination coefficient R². In addition, when the experimental adsorption capacity value were compared to those calculated using different model, the pseudo-secondorder model generated values that were in good agreement with the experimental results, while the pseudo-first-order model produced values that were found to be considerably different from the experimental ones. We contend that the chemisorption process is the ratelimiting phase since the adsorption process closely adhered to the pseudo-second-order model (Alizadeh et al., 2024). In this process, the adsorbent surface's adsorption sites' accessibility is the determining factor to affect the rate of adsorption for MB and PCT by PVA_PV-P_IC_30NPF. Furthermore, as illustrated in Fig. S8, the linear fitting results of the adsorption process are consistent with the intraparticle diffusion model. It was noticed that, two stages of the adsorption process were carried out for MB and PCT at low concentrations. The first stage's high fitting slope suggests that the adsorbent boundary layer is diffusing quickly. It appears that the adsorption mechanism is complex since the reduced effectiveness in the second stage matches the lower diffusion rate into hydrogel grains. On the other hand, for high starting concentration of MB and PCT, the adsorption process' linear fitting can be divided into three steps as shown in Fig. S8a. First, at high concentration, the molecules are transported in the bulk solution. Second, by either a diffusion process at the boundary layer or a diffusion of charged molecules from the bulk solution to the hydrogel's exterior surface, the charged molecules can enter the pores and/or intraparticle active sites of the hydrogel. Third, the charged molecules can diffuse through the pores of the hydrogel and undergo a chemical binding reaction before reaching the equilibrium. The slope of the liner fitting (k) indicates the rate of diffusion; a higher k value indicates a faster diffusion process. Therefore, k1 > k2 > k3 suggested that the available free path for diffusion decrease and the pore size decrease, which in turn caused the diffusion process's rate to drop. In earlier research, the interpretation of this phenomenon was also documented (Cheng et al., 2013).

The Freundlich, Langmuir, Temkin, and Dubinin-Redushkovic isotherm models were used to assess the absorbency of PVA_PV-P_IC_30NPF scaffold to remove MB and PCT cations from wastewater at different temperatures and starting concentrations to explain how the material and adsorbent adsorption interactions might occur (Fig. S9). The Langmuir model assumes that adsorption solely occurs on the surface and that there is no contact between adsorbents. This allows the model to explain the experimental data throughout a wide concentration range. On the other hand, the Freundlich model (model multilayer adsorption), which assumes that adsorption takes place at irregularly dispersed adsorption sites on the medium's surface (Akpomie and Conradie, 2023; Chen et al., 2023). In Table 2, it is seen that all R² values for Langmuir and Freundlich models are near to 1 or equal 1, so both model can represents the adsorption data. From the Langmuir model analysis, we estimated the maximum adsorption capacity values (q_m) again MB and PCT, respectively, at varying temperatures. From the perspective of physics, we favor the Freundlich model, where a

heterogeneous chemisorption process takes place. This mechanism is more consistent with the kinetic model of intraparticle diffusion and the finding that MB and PCT molecules mostly adsorbed onto PVA_PV-P_IC_30NPF hydrogel scaffold through the inner surface.

The average energy (ϵ) for the adsorption of MB and PCT cations was found to be 80,443 and 77,047 kJ. mol^{-1} , respectively, using the Dubinin-Redushkovic isotherm model. These values of ϵ are greater than 8 kJ mol^{-1} , confirming the presence of chemical bonds during the adsorption process (Foroutan et al., 2023b), and that was compliance with the data from the Temkin isotherm, as the values of A_T and b_T parameters showed that the chemosorption can also play a role in the MB and PCT removal using PVA_PVP_IC_30NPF hydrogel scaffold.

The influence of temperature on MB and PCT adsorption into PVA_PVP_IC_30NPF hydrogel scaffold was investigated and the findings are illustrated in Table 2. By rising temperature from 25–45 °C, the adsorption efficiency of MB and PCT increased from 66.5, and 89 % to 82, and 95.1 %, respectively. The increase in the adsorption efficiency with rising temperature can be caused by the increasing of activation energy that increase the activation of chemical bonding between the MB or PCT and scaffold. Thermodynamics parameters (Gibbs free energy: Δ G, entropy: Δ S, and enthalpy: Δ H) were calculated using Eqs. (7)–(9) to determine the type of adsorption process (endothermic or exothermic process) (Peighambardoust et al., 2024).

$$K_{D} = \frac{q_{e}}{C_{c}} \tag{7}$$

$$\Delta G = -RT \ln K_D \tag{8}$$

$$lnK_D = \frac{\Delta S}{R} - \frac{\Delta H}{RT} \tag{9}$$

R is the universal gas constant, T is the temperature in Kelven, K_D is the equilibrium constant of the adsorption process. ΔG values for MB and PCT were determined to be negative, confirming the spontaneity of the reaction. It should also be noted that the positive values of ΔH for MB and PCT adsorption process confirmed that the process is endothermic and chemical bonds occurred between pollutants molecules and the scaffold (Foroutan et al., 2023b) and its magnitude confirming its chemisorption nature whereas the ΔH values are >200 kJ mol⁻¹ (Tran et al., 2021). ΔS values for adsorption were positive, indicating a random collisions between absorbent and MB or PCT molecules.

One important factor that can verify the efficiency of adsorbent is its adsorption capability. The capacity and industrial applicability are important aspects to take into account. Table S8 lists the adsorption capacities of several green hydrogel composite used as absorbers for the removal of organic cations in comparison to the absorbers utilized in this investigation. The findings demonstrate that the PVA_PVP_IC_30NPF scaffold has a greater adsorption capacity than many of the absorbers utilized to remove those contaminants. As a result, the hydrogels that are generated can be used as suitable absorbers to extract various cations pollutants from aqueous systems.

3.6. Reusability test

The reusability and structural stability of the PVA_PVP_IC_30NPF hydrogel were evaluated during five adsorption—desorption cycles with a starting concentration of 50 mg $\rm L^{-1}$, pH 12 for MB and pH 7 for PCT, and temperature 25 °C. It is discovered that even after this continuous usage, the removal efficiency declining by less than six percent for MB and less than five percent for PCT as shown in Fig. 6. This performance is highly encouraging for the actual use of this hydrogel nanocomposite for industrial water filtration.

3.7. Life cycle assessment (LCA)

Despite the fact that natural fillers in polymeric matrixes possess

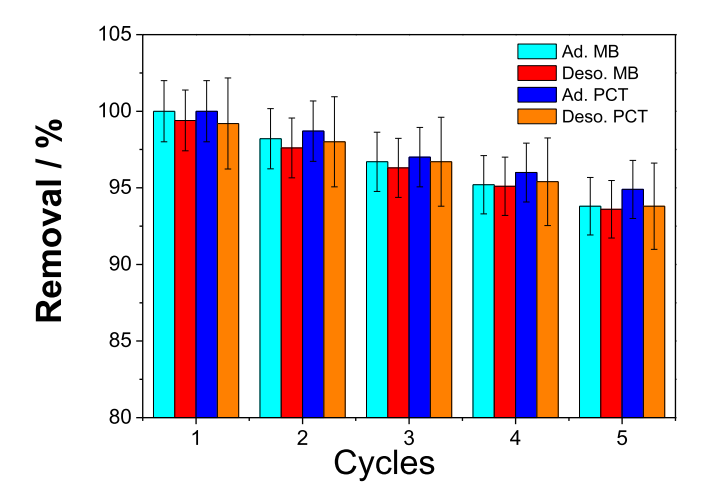


Fig. 6.: Reusability cycles of MB and PCT into PVA PVP IC 30NPF hydrogel.

industrial relevance, an examination must be conducted to confirm the environmental effects of the industrial waste utilized and all associated procedures. Therefore, life cycle assessment (LCA) is a useful tool for confirming the environmental impact of materials, assessing the sustainable application of date palm frond waste into the PVA_PVP_IC hydrogel matrix, and assessing the impact of the nanocomposite hydrogel adsorbent under environmental categories. As a result, the performance of the PVA PVP IC hydrogel was compared to the hydrogels matrix containing 10-30 wt% NPF. Furthermore, waste incineration is the most popular method of managing residues for wood waste which was taken into consideration to account for the situation in which the NPF was absent from the polymer matrix (Nabavi-Pelesaraei et al., 2017). As a result, a percentage dependent on the quantity of NPF added to the hydrogel matrix was taken into consideration to look into the process's effects on the environment. While a lesser amount of burned residue was taken into consideration for hydrogels containing NPF, all residue for PVA_PVP_IC was thought to be burned in order to generate energy (Rigamonti et al., 2020). The LCA results taking into account the most affected environmental categories such as water depletion, ozone depletion, fossil fuel depletion, and agricultural land occupation which are displayed in Fig. 7. Regarding the fossil depletion depicted in Fig. 7a, a reduction was noted as the amount of NPF in the blend polymer matrix increased. This observation may be related to the complex procedure involved in the creation of the hydrogels. Additionally, palm waste management can have a big impact because, when using conventional vehicles, waste transportation also burns fossil fuels. Consequently, compared to other environmental categories, the observed reduction was not as significant. However, as seen in Fig. 7b & c, the most affected categories were ozone depletion and agricultural land occupancy, since these categories are closely linked to the management of palm waste, they were severely impacted. Additionally, burning this palm waste produces a fair amount of gasses, which contribute to ozone depletion. For the water depletion category, an increase is associated with palm waste reevaluation and the increasing of water used during hydrogels preparation Fig. 7d.

4. Conclusions

A new hydrogel adsorbent nanocomposite for organic pollutants was demonstrated. This system is based on a crosslinked PVA, PVP, and IC infused with different ratios of nanoscale palm frond (NPF) particles. This nanocomposite hydrogel system was tested for the removal of MB and PCT cations at different concentrations, pH values and temperatures. Based on experimental results, the adsorption mechanism was found to be dominated by the electrostatic interactions, and chemical bonding occurred between the cationic groups of MB or PCT and the

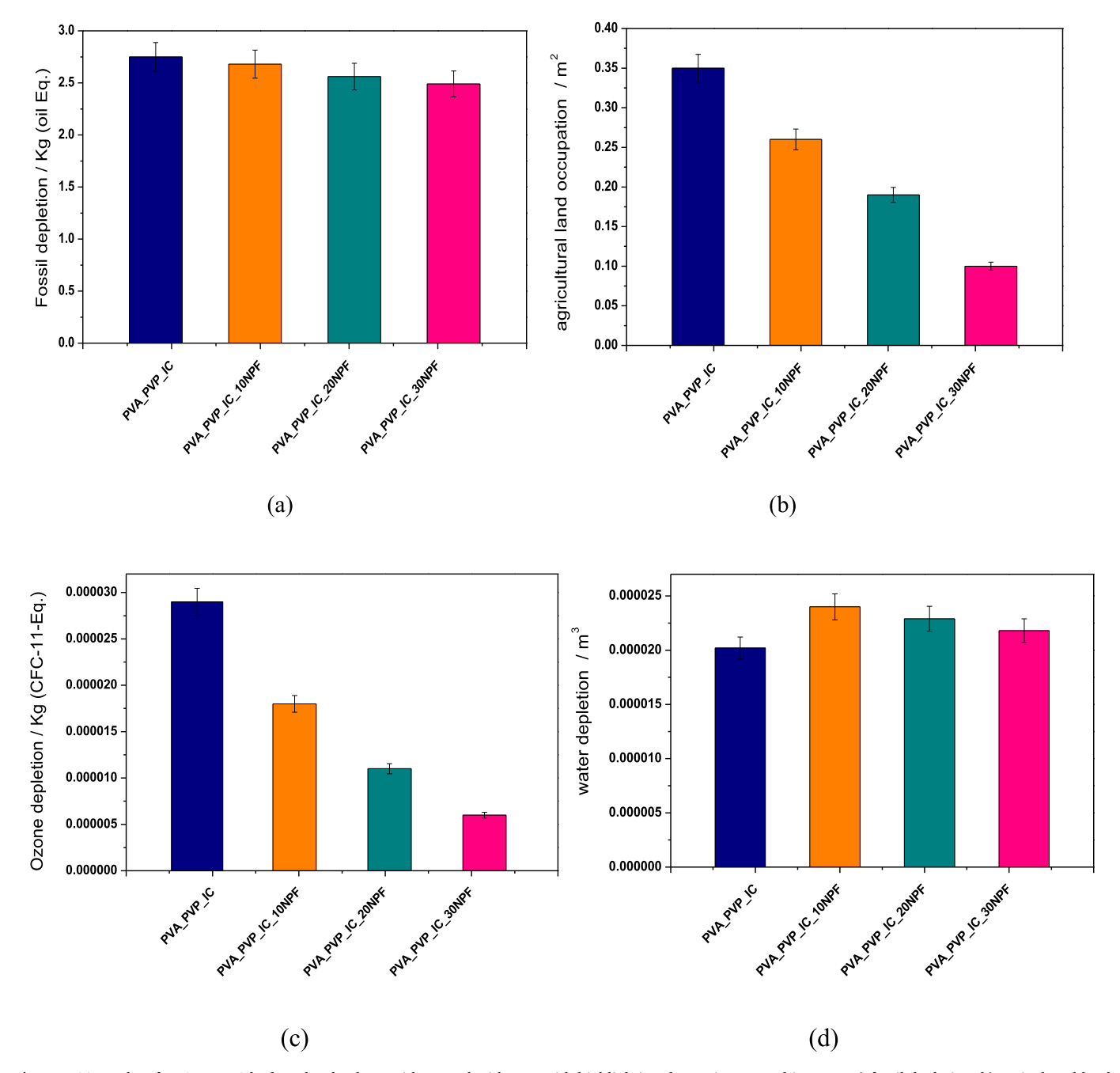


Fig. 7. LCA results of PVA_PVP_IC hydrogels adsorbent without and with NPF with highlighting the environmental impacts: a) fossil depletion; b) agricultural land occupation; c) ozone depletion; d) water depletion.

anionic groups of polymeric blend and NPF in the composite. By employing the RSM to optimize the removal efficiency of a hydrogel with 30 wt percent NPF. The complete removal efficiency could be reached for both pollutants at an adsorption time duration of 66.7 hr, 98.5 mg $\rm L^{-1}$ starting concentration, and an adsorbent dose of 5.9 mg for the MB removal; an adsorption time duration of 57.6 h, 80 mg $\rm L^{-1}$ starting concentration, and an adsorbent dose equal to 6 mg for the PCT removal. The analysis of PVA_PVP_IC_30NPF hydrogel absorbance using several kinetic models helped to clarify the removal mechanism, which confirmed the role of the physical and chemical sorption between the hydrogel and MB or PCT molecules. The Freundlich, Langmuir, Temkin, and Dubinin-Redushkovic isotherm models confirm the presence of a chemisorption process along with a physisorption process during the adsorption process of MB and PCT. However, according to the thermodynamics results, the adsorption process for both pollutants onto the

tested scaffold is spontaneity, endothermic, and a random collisions process. Five consecutive cycles of absorption and desorption were conducted to demonstrate the hydrogel containing 30 wt% of NPF has a good adsorption/desorption capability. The LCA demonstrated many environmental advantages as a result of the hydrogel composite's reduced polymer demand and decreased volume of date palm frond waste that would otherwise be incorrectly disposed of in the environment and have an adverse effect on the ecosystem. Based on the "wastestreat-wastes" strategy, this study demonstrates how waste-derived materials may be used in wastewater treatment to meet sustainability and efficient waste/water management objectives.

CRediT authorship contribution statement

Noha A. Elessawy: Writing - original draft, Methodology,

Investigation, Conceptualization. **Abdulrahman G. Alhamzani:** Validation, Formal analysis. **Sondos A.J. Almahmoud:** Validation, Formal analysis. **Benjamin S. Hsiao:** Writing – review & editing, Validation, Supervision.

Declaration of Competing Interest

The authors declare that they have no known competing financial interests or personal relationships that could have appeared to influence the work reported in this paper.

Data availability

Data will be made available on request.

Acknowledgment

The authors would like to thank and appreciate the Deanship of Scientific Research at Imam Mohammad Ibn Saud Islamic University (IMSIU) for funding through Research Partnership (grant number IMSIU-RP23052). BSH acknowledges that partial support by the National Science Foundation grant (NSF-DMR-2216585).

Appendix A. Supporting information

Supplementary data associated with this article can be found in the online version at doi:10.1016/j.ecoenv.2024.117123.

References

- Ahmad, T., Danish, M., Rafatullah, M., Ghazali, A., Sulaiman, O., Hashim, R., Ibrahim, M.N.M., 2012. The use of date palm as a potential adsorbent for wastewater treatment: a review. Environ. Sci. Pollut. Res 19, 1464–1484. https://doi.org/ 10.1007/s11356-011-0709-8".
- Ahmed, E.M., 2015. Hydrogel: preparation, characterization, and applications: a review. J. Adv. Res. 6 (2), 105–121. https://doi.org/10.1016/j.jare.2013.07.006.
- Akpomie, K.G., Conradie, J., 2023. Efficient adsorptive removal of paracetamol and thiazolyl blue from polluted water onto biosynthesized copper oxide nanoparticles. Sci. Rep. 13, 859. https://doi.org/10.1038/s41598-023-28122-0.
- Al Haddabi, M., Ahmed, M., Al Jebri, Z., Vuthaluru, H., Znad, H., Al Kindi, M., 2016. Boron removal from seawater using date palm (Phoenix dactylifera) seed ash. Desalin. Water Treat. 57, 5130–5137.
- Al-Ghamdi, A., Altaher, H., Omar, W., 2013. Application of date palm trunk fibers as adsorbents for removal of Cd+2 ions from aqueous solutions. J. Water Reuse Desalin. 3, 47–54.
- Alizadeh, M., Peighambardoust, S.J., Foroutan, R., 2024. Efficacious adsorption of divalent nickel ions over sodium alginate-g-poly (acrylamide)/hydrolyzed Luffa cylindrica-CoFe₂O₄ bionanocomposite hydrogel. Int. J. Biol. Macromol. 254, 127750. https://doi.org/10.1016/j.ijbiomac.2023.127750.
- Alizadeh, M., Peighambardoust, S.J., Foroutan, R., Azimi, H., Ramavandi, B., 2022. Surface magnetization of hydrolyzed Luffa Cylindrica biowaste with cobalt ferrite nanoparticles for facile Ni2+ removal from wastewater. Environ. Res. 212, 113242. https://doi.org/10.1016/j.envres.2022.113242.
- Amin, M.T., Alazba, A.A., Amin, M.N., 2016. Absorption behaviours of copper, lead, and arsenic in aqueous solution using date palm fibres and orange peel: Kinetics and thermodynamics. Pol. J. Environ. Stud. 26, 543–557.
- Ashour, S.S., 2010. Kinetic and equilibrium adsorption of methylene blue and remazol dyes onto steam-activated carbons developed from date pits. J. Saudi Chem. Soc. 14 (1), 47–53. https://doi.org/10.1016/j.jscs.2009.12.008.
- Bashir, S., Hina, M., Iqbal, J., Rajpar, A.H., Mujtaba, M.A., Alghamdi, N.A., Wageh, S., Ramesh, K., Ramesh, S., 2020. Fundamental concepts of hydrogels: synthesis, properties, and their applications. Polymers 12 (11), 2702. https://doi.org/10.3390/ polym12112702.
- Box, G., Behnken, D.W., 1960. Some new three level designs for the study of quantitative variables. Technometrics 2, 455–475.
- Chang, H., Zhao, H., Qu, F., Yan, Z., Liu, N., Lu, M., Liang, Y., Lai, B., Liang, H., 2023. State-of-the-art insights on applications of hydrogel membranes in water and wastewater treatment. Sep. Purif. Technol. 308, 122948.
- Chen, K., Li, Y., Wang, M., Du, Q., Sun, Y., Zhang, Y., Chen, B., Jing, Z., Jin, Y., Zhao, S., 2023. Removal of methylene blue dye from aqueous solutions by pullulan polysaccharide/polyacrylamide/activated carbon complex hydrogel adsorption. ACS Omega 8 (1), 857–867. https://doi.org/10.1021/acsomega.2c06205.
- Cheng, C., Deng, J., Lei, B., He, A., Zhang, X., Ma, L., Li, S., Zhao, C., 2013. Toward 3D graphene oxide gels based adsorbents for high-efficient water treatment via the promotion of biopolymers. J. Hazard. Mater. 263, 467–478. https://doi.org/10.1016/j.jhazmat.2013.09.065.

- Correa, S., Grosskopf, A.K., Hernandez, H.L., Chan, D., Yu, A.C., Stapleton, L.M., Appel, E.A., 2021. Translational applications of hydrogels. Chem. Rev. 121, 11385–11457. https://doi.org/10.1021/acs.chemrev.0c01177.
- Elessawy, N.A., Gouda, M.H., Elkady, M.F., Ali, S.M., Gouda, M., Mohy Eldin, M.S., 2020. Ultra-fast removal of cadmium and lead from wastewater using high-efficient adsorbent derived from plastic waste: Statistical modeling kinetic and isotherm studies. Desalin. Water Treat. 173, 394–408. https://doi.org/10.5004/ dwt.2020.24809.
- Elessawy, N.A., Gouda, M.H., Elnouby, M., Ali, S.M., Salerno, M., Youssef, M.E., 2022. Sustainable microbial and heavy metal reduction in water purification systems based on PVA/IC nanofiber membrane doped with PANI/GO. Polymers 14, 1558. https://doi.org/10.3390/polym14081558.
- Faiad, A., Alsmari, M., Almed, M.M.Z., Bouazizi, M.L., Alzahrani, B., Alrobei, H., 2022. Date palm tree waste recycling: treatment and processing for potential engineering applications. Sustainability 14, 1134. https://doi.org/10.3390/su14031134.
- Foroutan, R., Khoo, F.S., Ramavandi, B., Abbasi, S., 2017. Heavy metals removal from synthetic and shipyard wastewater using Phoenix dactylifera activated carbon. Desalin. Water Treat. 82, 146–156. https://doi.org/10.5004/dwt.2017.20908.
- Foroutan, R., Mohammadi, R., Taheri, M., Ahmadi, A., Ramavandi, B., 2023a. Edible waste oil to biofuel using reclaimable g-C3N4/HAp/Fe3O4/ K2CO3 nanobiocomposite catalyst: Toxicity evaluation and optimization. Environ. Technol. Innov. 32, 103403. https://doi.org/10.1016/ji.eti.2023.103403.
- Foroutan, R., Peighambardoust, S.J., Ghojavand, S., Farjadfard, S., Ramavandi, B., 2023b. Cadmium elimination from wastewater using potato peel biochar modified by ZIF-8 and magnetic nanoparticle. Colloid Interface Sci. Commun. 55, 100723. https://doi.org/10.1016/j.colcom.2023.100723.
- Fseha, Y.H., Shaheen, J., Sizirici, B., 2023. Phenol contaminated municipal wastewater treatment using date palm frond biochar: Optimization using response surface methodology. Emerg. Contam. 9, 100202. https://doi.org/10.1016/j. emcon.2022.100202.
- Ghosh, N., Sen, S., Biswas, G., Singh, L.R., Chakdar, D., Haldar, P.K., 2022.
 A comparative study of CuO nanoparticle and CuO/PVA-PVP nanocomposite on the basis of dye removal performance and antibacterial activity in wastewater treatment.
 Int. J. Environ. Anal. Chem. 1–21. https://doi.org/10.1080/03067319.2022.2060088.
- Gouda, M.H., Ali, S.M., Othman, S.S., Abd Al-Aziz, S.A., Abu-Serie, M.M., Elsokary, N.A., Elessawy, N.A., 2021b. Novel scaffold based graphene oxide doped electrospun iota carrageenan/polyvinyl alcohol for wound healing and pathogen reduction: in-vitro and in-vivo study. Sci. Rep. 11, 20456. https://doi.org/10.1038/s41598-021-00069-0
- Gouda, M.H., Elessawy, N.A., Santos, D.M.F., 2020a. Synthesis and characterization of novel green hybrid nanocomposites for application as proton exchange membranes in direct borohydride fuel cells. Energies 13, 1180. https://doi.org/10.3390/ en13051180.
- Gouda, M.H., Elessawy, N.A., Elnouby, M., Ghorab, M.A., Radwan, I.O., Hashim, A., Youssef, M.E., Santos, D.M.F., 2022. Evaluation of sulfonated chitosan-g-sulfonated polyvinyl alcohol/polyethylene oxide/sulfated zirconia composite polyelectrolyte membranes for direct borohydride fuel cells: Solution casting against the electrospun membrane fabrication technique. Front. Mater. 9. https://doi.org/10.3389/ fmats.2022.912006.
- Gouda, M.H., Gouveia, W., Afonso, M.L., Sljukic, B., El Essawy, N.A., Nassr, A.B.A.A., Santos, D.M.F., 2019. Poly(vinyl alcohol)-based crosslinked ternary polymer blend doped with sulfonated graphene oxide as a sustainable composite membrane for direct borohydride fuel cells. J. Power Sources 432, 92–101. https://doi.org/ 10.1016/j.jpowsour.2019.05.078.
- Gouda, M.H., Gouveia, W., Elessawy, N.A., Šljukić, B., Nassr, A.B.A.A., Santos, D.M.F., 2020b. Simple design of PVA-based blend doped with SO4(PO4)-functionalised TiO2 as an effective membrane for direct borohydride fuel cells. Int. J. Hydrogen Energy 45, 15226–15238.
- Gouda, M.H., Konsowa, A.H., Farag, H.A., Elessawy, N.A., Tamer, T.M., Mohy Eldin, M. S., 2021a. Development novel eco-friendly proton exchange membranes doped with nano sulfated zirconia for direct methanol fuel cells. J. Polym. Res 28, 263. https://doi.org/10.1007/s10965-021-02628-5.
- Gupta, S., Saud, A., Munira, N., Allal, A., Preud'homme, H., Shomar, B., Zaidi, S.J., 2024.
 Removal of heavy metals from wastewater by aerogel derived from date palm waste.
 Environ. Res. 245, 118022. https://doi.org/10.1016/j.envres.2023.118022.
- Hassan, S.S., Al-Ghouti, M.A., Abu-Dieyeh, M., McKay, G., 2020. Novel bioadsorbents based on date pits for organophosphorus pesticide remediation from water. J. Environ. Chem. Eng. 8, 103593. https://doi.org/10.1016/j.jece.2019.103593.
- Jozaghkar, M.R., Azar, A.Š., Žiaee, F., 2022. Preparation, Characterization, and swelling study of N,N'-dimethylacrylamide/acrylic acid amphiphilic hydrogels in diferent conditions. Polym. Bull. 79, 5183–5195. https://doi.org/10.1007/s00289-021-02726_d!"
- Khiewsawai, N., Rattanawongwiboon, T., Tangwongputti, C., Ummartyotin, S., 2023. Preparation of cellulose fiber derived from sugarcane bagasse and polyvinyl alcohol (PVA)-based hydrogel composite by gamma irradiation as a platform for colorimetric sensor. Emergent Mater. 6, 2041–2052. https://doi.org/10.1007/s42247-023-00577-x
- Liu, X., Liu, J., Lin, S., Zhao, X., 2020. Hydrogel machines. Mater. Today 36, 102–124. https://doi.org/10.1016/j.mattod.2019.12.026.
- Mahdavinia, G.R., Mousanezhad, S., Hosseinzadeh, H., Darvishi, F., Sabzi, M., 2016.Magnetic hydrogel beads based on PVA/sodium alginate/laponite RD and studying their BSA adsorption. Carbohydr. Polym. 147, 379–391.
- Mahdi, Z., Yu, Q.J., El Hanandeh, A., 2018. Removal of lead(II) from aqueous solution using date seed-derived biochar: batch and column studies. Appl. Water Sci. 8, 181

- Marton, A.M.S., Monticeli, F.M., Zanini, N.C., Barbosa, R.F.S., Medeiros, S.F., Rosa, D.S., Mulinari, D.R., 2022. Revalorization of Australian royal palm (Archontophoenix alexandrae) waste as reinforcement in acrylonitrile butadiene styrene (ABS) for use in 3D printing pen. J. Clean. Prod. 365, 132808. https://doi.org/10.1016/j.iclenro.2022.132808
- Nabavi-Pelesaraei, A., Bayat, R., Hosseinzadeh-Bandbafha, H., Afrasyabi, H., Chau, K., 2017. Modeling of energy consumption and environmental life cycle assessment for incineration and landfill systems of municipal solid waste management - a case study in Tehran Metropolis of Iran. J. Clean. Prod. 148, 427–440. https://doi.org/ 10.1016/j.jclepro.2017.01.172.
- Olad, A., Doustdar, F., Gharekhani, H., 2020. Fabrication and characterization of a starch-based superabsorbent hydrogel composite reinforced with cellulose nanocrystals from potato peel waste. Colloids Surf. A 601, 124962.
- Peighambardoust, S.J., Boffito, D.C., Foroutan, R., Ramavandi, B., 2022. Sono-photocatalytic activity of sea sediment@400/ZnO catalyst to remove cationic dyes from wastewater. J. Mol. Liq. 367, 120478. https://doi.org/10.1016/j.mollid.2022.120478.
- Peighambardoust, S.J., Zardkhaneh, S.I., Foroughi, M., Foroutan, R., Azimi, H., Ramavandi, B., 2024. Effectiveness of polyacrylamide-g-gelatin/ACL/Mg-Fe LDH composite hydrogel as an eliminator of crystal violet dye. Environ. Res. 258, 119428. https://doi.org/10.1016/j.envres.2024.119428.
- Pooladi, H., Foroutan, R., Esmaeili, H., 2021. Synthesis of wheat bran sawdust/Fe3O4 composite for the removal of methylene blue and methyl violet. Environ. Monit. Assess. 193, 276. https://doi.org/10.1007/s10661-021-09051-9.
- Rambabu, K., Bharath, G., Avornyo, A., Thanigaivelan, A., Hai, A., Banat, F., 2023. Valorization of date palm leaves for adsorptive remediation of 2,4-dichlorophenoxyacetic acid herbicide polluted agricultural runoff. Environ. Pollut. 316 (Part 2), 120612. https://doi.org/10.1016/j.envpol.2022.120612.
- Rashid, R., Shafiq, I., Akhter, P., Iqbal, M., Hussain, M., 2021. A state-of-the-art review on wastewater treatment techniques: the effectiveness of adsorption method. Environ. Sci. Pollut. Res 28, 9050–9066.
- Rigamonti, L., Taelman, S.E., Huysveld, S., Sfez, S., Ragaert, K., Dewulf, J., 2020. A step forward in quantifying the substitutability of secondary materials in waste management life cycle assessment studies. Waste Manag 114, 331–340. https://doi. org/10.1016/j.wasman.2020.07.015.
- Romdhani, M., Attia, A., Charcosset, C., Mahouche-Chergui, S., Ates, A., Duplay, J., Ben Amar, R., 2023. Optimization of paracetamol and chloramphenicol removal by novel activated carbon derived from sawdust using response surface methodology. Sustainability 15, 2516.
- Salem, I.B., Saleh, M.B., Iqbal, J., El Gamal, M., Hameed, S., 2021. Date palm waste pyrolysis into biochar for carbon dioxide adsorption. Energy Rep. 7, 152–159.
- Salunkhe, B., Schuman, T.P., 2021. Super-adsorbent hydrogels for removal of methylene blue from aqueous solution: dye adsorption isotherms, kinetics, and thermodynamic properties. Macromol 1, 256–275. https://doi.org/10.3390/macromol1040018.

- Saud, A., Saleem, H., Khan, A.W., Munira, N., Khan, M., Zaidi, S.J., 2023. Date palm tree leaf-derived cellulose nanocrystal incorporated thin-film composite forward osmosis membranes for produced water treatment. Membranes 13, 513.
- Shaheen, T.I., El-Shahat, M., Abdelhameed, R.M., 2022. Size-tunable effect of CaCO3/nanocellulose hybrid composites on the removal of paracetamol from aqueous solution. Environ. Sci. Pollut. Res. 29, 43287–43299.
- Siva Kumar, N., Asif, M., Poulose, A.M., Al-Ghurabi, E.H., Alhamedi, S.S., Koduru, J.R., 2023. Preparation, characterization, and chemically modified date palm fiber waste biomass for enhanced phenol removal from an aqueous environment. Materials 16, 4057. https://doi.org/10.3390/ma16114057.
- Sizirici, B., Fseha, Y.H., Yildiz, I., Delclos, T., Khaleel, A., 2021. The effect of pyrolysis temperature and feedstock on date palm waste derived biochar to remove single and multi-metals in aqueous solutions. Sustain. Environ. Res. 31, 9.
- Spagnol, C., Rodrigues, F.H.A., Neto, A.G.V.C., Pereira, A.G.B., Fajardo, A.R., Radovanovic, E., Rubira, A.F., Muniz, E.C., 2012. Nanocomposites based on poly (acrylamide- co-acrylate) and cellulose nanowhiskers. Eur. Polym. J. 48, 454–463.
- Tahir, A.H.F., Al-Obaidy, A.M.J., Mohammed, F.H., 2020. Biochar from date palm waste, production, characteristics and use in the treatment of pollutants: a review. IOP Conf. Ser.: Mater. Sci. Eng. 737, 012171. https://doi.org/10.1088/1757-899X/737/1/012171
- Toghan, A., Gouda, M.H., Zahran, H.F., Alakhras, A.I., Sanad, M.M.S., Elessawy, N.A., 2023. Development of a new promising nanocomposite photocatalyst of polyaniline/ carboxylated graphene oxide supported on PVA film to remove different ecological pollutants. Diam. Relat. Mater. 139, 110400.
- Tran, N.H., Lima, E.C., Juang, R., Bollinger, J., Chao, H., 2021. Thermodynamic parameters of liquid-phase adsorption process calculated from different equilibrium constants related to adsorption isotherms: a comparison study. J. Environ. Chem. Eng. 9, 106674. https://doi.org/10.1016/j.jece.2021.106674.
- Tran, V.V., Park, D., Lee, Y.C., 2018. Hydrogel applications for adsorption of contaminants in water and wastewater treatment. Environ. Sci. Pollut. Res. 25 (25), 24569–24599. https://doi.org/10.1007/s11356-018-2605-y.
- Weber, E.J., Wolfe, N.L., 1987. Kinetics studies of reduction of aromatic azo compounds in anerobic sediment/water systems. Environ. Toxicol. Chem. 6, 911–919. https://doi.org/10.1002/etc.5620061202.
- Wu, S., Shi, W., Li, K., Cai, J., Xu, C., Gao, L., Lu, J., Ding, F., 2023. Chitosan-based hollow nanofiber membranes with polyvinylpyrrolidone and polyvinyl alcohol for efficient removal and filtration of organic dyes and heavy metals. Int. J. Biol. Macromol. 239, 124264. https://doi.org/10.1016/j.ijbiomac.2023.124264.
- Xu, Z., Wei, C., Jin, J., Xu, W., Wu, Q., Gu, J., Ou, M., Xu, X., 2018. Development of a novel mixed titanium, silver oxide polyacrylonitrile nanofiber as a superior adsorbent and its application for MB removal in wastewater treatment. J. Braz. Chem. Soc. 29, 560–571.
- Ye, Y.S., Rick, J., Hwang, B.J., 2012. Water soluble polymers as proton exchange membranes for fuel cells. Polymers 4, 913–963. https://doi.org/10.3390/ polym4020913.